

A Segmentation Method For Multi-Connected Particle Delineation

Xingqiang Wu, John M. Kemeny

Department of Mining and Geological Engineering
University of Arizona, Tucson AZ 85721

Abstract

An automatic particle segmentation system is developed for calculating the size distribution of rock fragments created by blasting. A rock composite due to blasting is often fully multi-connected in which individual particles can not be delineated by the existing segmentation algorithms. Two algorithms are proposed to approach this multi-connected segmentation problem. The first algorithm analyzes the shape of each shadow (a simply-connected region) and "splits" the particles from shadow boundary convexity points if a relatively large gradient path occurs. The second algorithm finds clusters of rock particles which may not be delineated due to the lack of a strong gradient along the touching portions and delineates them using a shape heuristics. A large number of test results show that the method is fast and accurate.

I. Introduction

Predicting the level and extent of rock fragmentation from blasting is important for many operations in the mining industry. For the processing of certain minerals, for instance, the rock fragments following blasting must be further reduced in size, and minimizing the fragment sizes from blasting can result in a significant reduction in crushing and grinding costs. For other minerals, the rock fragments following blasting are placed in piles for leaching, and the size distribution of the rock fragments in the piles determines the efficiency of mineral recovery. There are many traditional methods to estimate the size distribution of blasted rocks. The most direct method is to sieve the blasted rocks through screens with different mesh sizes [1]. The high cost of doing this for tons of blasted material has led to many indirect methods for estimating the size distributions. One of the popular methods is photoanalysis, where photographic images are obtained from the surface of a pile of blasted rocks and analyzed either by hand or through computer image processing

techniques [2], [3], [4].

A photographic image of rock fragments due to blasting is shown in Fig. 1. In order to calculate the size distribution from such an image, the computer must first recognize the individual rock particles. Fig. 1 illustrates many of the problems encountered in trying to "split" or delineate individual rock particles. First of all, shadows fill the void spaces between rock fragments, and also partially along the edges of fragments. Noise is also present due to the complex texture of the rock, as well as surface roughness. The rock particles overlap and touch, making it difficult to completely detect particle edges. Finally, the size of the rock particles in an image may range from very small to very large, making it difficult to differentiate the small particles from noise on the large particles. Methods to recognize touching individual rock particles have been developed by Maerz *et al* [5], Gao and Wong [6]. These approaches which are primarily based on edge detection techniques are sensitive to noise, and require hand editing under many circumstances.

Methods appropriate for particle delineation have also been developed in other fields such as the biomedical area, using methods such as heuristic search [7], fuzzy set theory [8], region growing [9], [10] and intelligent splitting [11]. These segmentation methods are mostly based on the assumption that the particles to be delineated are simply-connected. In particular, images of rock fragments contain void areas due to porosity. This makes the problem multi-connected. The algorithms above can not be simply extended to solve fully multi-connected particle delineation problems. In this paper we describe a procedure for dealing with multi-connected touching objects. Once the individual rock particles have been delineated, the three-dimensional size distribution can be calculated using stereological techniques [12], [13].

In the following sections, a new procedure is described for multi-connected particle delineation problems. Using this procedure, nearly all touching rock particles can be automatically and accurately delineated. The rest of the paper is organized as follows: Section II describes

characteristics of images with touching particles. These features will form the basis for two delineation algorithms. Section III describes an algorithm for multi-connected particle delineation. Section IV describes the second delineation algorithm for simply-connected particle cluster regions. Section V briefly describes the calculation of size distribution of delineated rock particles. Section VI summarizes this research and presents our conclusions and plans for future work.

II Image understanding and assumptions

A characteristic of fragmented rocks is the large percentage of the volume taken up by void space or porosity (10-40%). Under natural light, these void areas will appear as dark or shaded areas. These dark areas will partially but not completely outline the boundaries of the rock fragments. In particular, where the shadow regions meet with particle edges, the shadow regions will form sharp convex shapes with angles that point in the direction of the edge between the touching particles (see Fig. 1). Also, in the region where the rock fragments touch, there usually will be relatively large gray level differences due to the particle edges. In almost all cases, there is at least some gray level difference between touching rock particles.

Since all rock particles touch and overlap each other in Fig. 1, all shadow regions must be separated by particles. Thus, we have the following lemma:

Lemma 1: If an image contains two types of regions,

and if one type of region is fully multi-connected, the other must be simply-connected.

Based on lemma 1, two algorithms are developed. The first algorithm extracts all shadow regions and analyzes the shapes of shadow regions and searches for large gradient paths in the region ahead of sharp convexities. The basis for algorithm 1 is as follows:

- (1) The shadow regions to be extracted are simply-connected;
- (2) The shadow boundary between particles tends to form convex areas that point in the direction of particle edges;
- (3) The gradient values along the touching areas of particles are larger than those in individual particle regions;
- (4) The particles under consideration are larger than some noise threshold.

Algorithm 2 will be used to find clusters of undelineated touching particles whose gradient values along the touching areas are almost the same as or less than those in individual particle regions (i.e., where assumption 2 above does not hold.) and delineate touching particles using a heuristic search. The basis for algorithm 2 is as follows:

- (1) Cluster regions of touching particles are simply-connected.
- (2) A cluster boundary at points where rock particles touch tends to form concave areas.
- (3) The touching length between two touching particles is relatively short compared with each individual particle perimeter on the either side of the touching path.



Fig. 1 A test image, bar in photo is 1 inch

III. Delineation algorithm 1

Due to the complex nature of the rock fragmentation problem, a two-stage procedure has been developed to delineate individual rock particles. The first algorithm analyzes the shapes of individual simply-connected shadow regions and makes all possible links between shadows. The shadow regions will become multi-connected and the particle regions simply-connected after algorithm 1. Most of the rock particles can be successfully delineated using algorithm 1. There are three major steps in algorithm 1. The first step is to extract a contour map for each of the shadow regions. Secondly, the interpolated angle and direction of the shadow boundary is calculated at each of the boundary points. The third step is to find connecting paths in neighboring shadows which pass through relatively large gradient areas. By deleting points along these paths, delineation lines are obtained. This procedure is repeated for all shadow contours in the image.

A. Gradient computation and shadow contour map

The two important features of a gray-level image which give information on the outline of individual rock particles are the shadows and the gradient in gray level from pixel to pixel. The gradients for every pixel are initially calculated

and saved for later use. Secondly, the proper threshold is applied to the original image to get a binary image and extract shadow contours from the binary image.

For each pixel in the image, its gradient is computed from the gray levels of its eight immediate neighboring pixels [15]. Table 1 shows pixel (i,j) with gray level f(i,j) along with its eight neighboring pixels:

f(i-1, j-1)	f(i-1, j)	f(i-1, j+1)
f(i, j-1)	f(i, j)	f(i, j+1)
f(i+1, j-1)	f(i+1, j)	f(i+1, j+1)

Table 1 Pixel(i,j) and its neighboring pixels

The gradient magnitude g(i,j) is as follows:

$$h(i,j) = f(i-1, j+1) - f(i-1, j-1) + 2f(i, j+1) - 2f(i, j-1) + f(i+1, j+1) - f(i+1, j-1)$$

$$v(i,j) = f(i+1, j-1) - f(i-1, j-1) + 2f(i+1, j) - 2f(i-1, j) + f(i+1, j+1) - f(i-1, j+1)$$

$$g(i,j) = \sqrt{h^2(i,j) + v^2(i,j)}$$

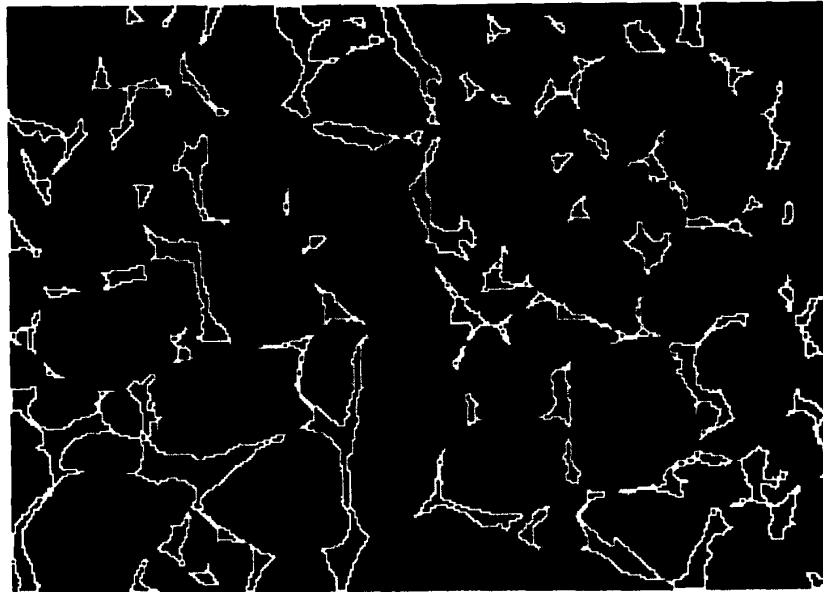


Fig. 2 Shadow contour image

In order to extract simply-connected shadow regions, an optimal threshold value which can preserve as much particle information as possible is selected, and a binary image is obtained. Using the contour encoding method [14], each black region is extracted from the binary image and then this 2-D black region is converted into a collection of 1-D boundary traces which contain a list of consecutive pixels along the shadow boundary. At the same time, very tiny black regions which are assumed to be noise are filled with white pixels. Fig. 2 shows the shadow contours for the test image.

B. Shadow convexities and directions

For each shadow boundary trace, curvatures and directions are computed at all boundary points, which will determine at where and in what direction two particles touch each other.

A shadow boundary is a 4-connected discrete pixel to pixel contour. Following Pavlidis [16], the procedure of calculating shadow boundary curvature is as follows: The "m-curvature" can be defined as the radius of a circle through P_i and neighbors m arc points away on either side.

Fig. 3 illustrates the calculation of 5-curvature. d is the distance to line $P_i P_{i+5}$, and r is the radius of the circle.

For small angle β ,

$$\sin\left(\frac{\beta}{2}\right) = \frac{\beta}{2}$$

thus

$$r \frac{\beta}{2} = \frac{d}{2}, \quad \beta = \frac{d}{r} = dk$$

where k is the curvature. Obviously, β is proportional to κ if d is fixed. Therefore, the angular separation between the directions of either side points can be used as a measure of curvature at the center point. For our purpose, the error in using β to estimate κ can be ignored, since only curvature comparisons rather than the absolute curvature value is needed. The shadow boundary points will be classified as convexity points or not, depending on the angle β of each boundary point.

The direction for each angle has to be defined so the initial searching direction from an initial search point can be obtained. The coordinates are set as shown in Fig. 3. The direction of the angle $P_{i-5}P_iP_{i+5}$ can be defined by the angle between the bisector of the angle $P_{i-5}P_iP_{i+5}$ and the y-axis.

For small shadows, especially when the perimeter of a shadow boundary is shorter than $2d$ for angle or 2κ for κ -curvature [17], the definition of angle does not make sense. The shape of a small shadow boundary will usually

be convex. Every point has to be checked to see if there is a relatively large gradient path to connect to another shadow boundary. An initial searching direction is defined as follows: find the center point of a small shadow region and choose this point as a reference point; the direction from the reference point to each boundary point is the initial searching direction of that boundary point. This is shown in Fig. 4.

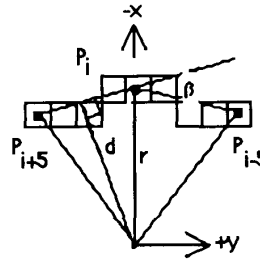


Fig. 3

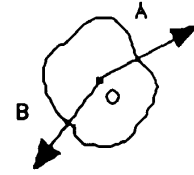


Fig. 4

Fig. 3 Angle and curvature

Fig. 4 Searching direction for small shadow

C. Searching route

The searching routine can be summarized as follows:

(1) Initial searching points: A list is made of all search points, denoted by Q , from a shadow boundary trace, denoted by \overline{S} . In the list, the angles of all points, denoted by A , that are larger than some convex angle threshold are denoted by T_A . So the following formula for Q will hold:

$$Q = \{ \text{Initial search points} \mid Q \in \overline{S}, A(Q) \geq T_A \}$$

For a small shadow, the angles of all points in \overline{S} are larger than T_A , and the above formula will reduce to:

$$Q = \{ \text{Initial search points} \mid Q \in \overline{S} \}$$

If there are N shadows, N lists of Q have to be made.

(2) The direction of the searching path: For each point in Q , the direction of this point is chosen as the initial searching direction. Then a search is made into R , which is an 8-connected subset of the discrete (x,y) plane that represents a cluster of fragmented rocks. In order to find the best connection path which is assumed to have local largest gradient pixels around the touching area, the searching direction will be recomputed after a few of pixels are searched. If the present pixel in the path is P_S , then the direction from P_{S-n} to P_S is the new direction. The

searching direction is recomputed after every n pixels. This is shown in Fig. 5.

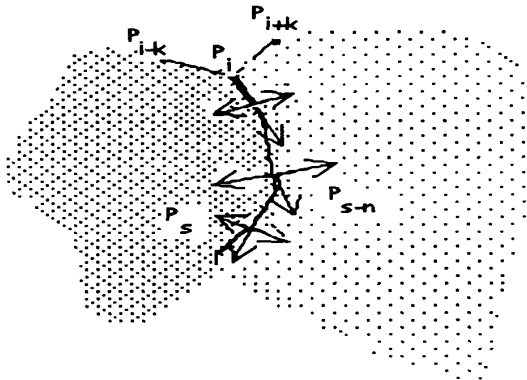


Fig. 5 Searching direction

(3) Searching window in the path: At the points which have different searching directions in the path, the local largest gradient pixel has to be chosen within a prescribed searching window, denoted by S_W . As shown in Figure 5, the searching window S_W is defined as the range that the distance from the points is not more than 3 pixels in the searching direction and not more than 3 pixels in the perpendicular direction. Every searching window S_W should be in R , i.e., $S_W \subset R$.

(4) Searching criterion: At the points which have different searching directions, the next point of the searching path is found which is the largest gradient pixel within the searching window S_W . If the largest gradient is greater than some gradient threshold T_G , this point will be the next searching start point in the path. The search then starts again from the next point. Otherwise, this searching path is given up and the algorithm continues with the next initial search point in Q . The following formula will hold for a searched path P :

$$P = \{ \text{Delineation line} \mid P \subset R, \overline{G}(P) \geq T_G \}$$

The searching continues until another shadow boundary is reached. If that boundary point is not in that search point list, this path is also given up and the algorithm continues with the next search point in Q .

(5) Particle shape criterion: When a delineation line has been completely searched, a particle shape criterion will be used to make final decision if the searched path is true or false. The length of the searched path from the initial search point to the end point should be less than the maximum distance from the points in the path to the boundary points of particles on the either side along the

path. If the above criterion is satisfied, a true delineation line is obtained.

(6) Repeat: Repeat the above steps for all initial search points in all lists of Q until no initial search points are left.

IV. Delineation algorithm 2

In general, most of the individual rock particles can be separated using the first algorithm. However, sometimes a few touching rock particles remain which have not been delineated due to the lack of a relatively large gradient path around the touching area. This algorithm is developed to check all of the particle regions which have already been processed by the first algorithm to find all possible clusters which include undelineated touching particles and delineate them.

A. Delineation route

This algorithm can be outlined as follows:

(1) A critical point: Using the same approach of a shadow boundary curvature analysis, the concavity of a cluster boundary is analyzed to make a list of concavity points in which the angles are less than some concave angle threshold. The most concave point in the list is chosen as a critical point which is supposed to be the intersection point of two touching rock particles.

(2) A pair of start and end points: A pair of start and end points from which a delineation line will be made are determined according to the following two criteria:

(a) The direction of the end point should be in the opposite of the direction of the start point.

(b) The distance from the start point to the end point should be less than 20% of the perimeter of the individual rock particle or cluster on the either side of the delineation line.

(3) Criterion of a cluster: if there are a pair of start and end points or more on a particle region boundary, the boundary is a cluster boundary. By deleting all pixels along the path from the start point to the end point, a delineation line is made. Otherwise, this region is made up of only an individual particle.

(4) Repeat: All of particle regions are checked to find possible cluster regions and delineate unseparated touching rock particles.

B. Final result after two algorithms

Fig. 6 shows the result of applying two delineation algorithms to the test image. The particles that are delineated using algorithm 2 are shaded.

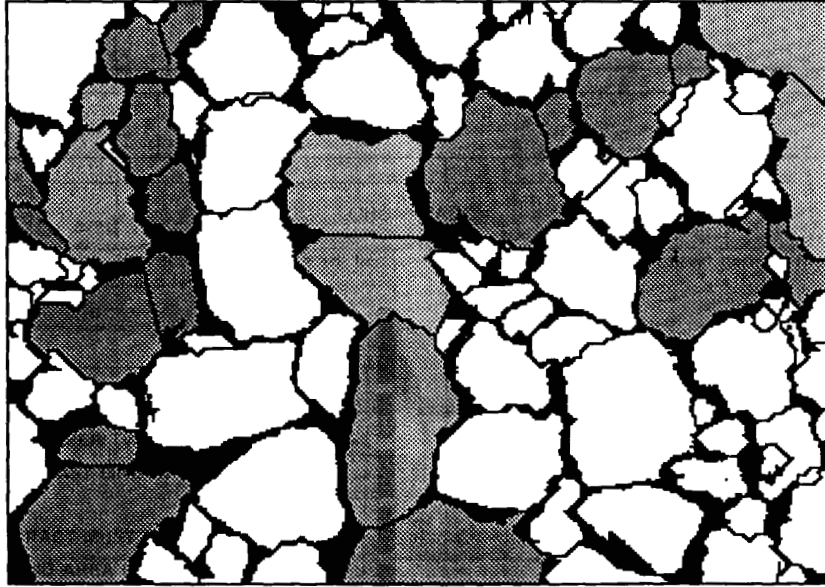


Fig. 6 Result. Shaded particles are delineated using algorithm 2.

V. Calculation of the particle size distribution

The particle delineation procedure outlined in this paper is a first step in calculating the size distribution of rock fragments in a volume of rock. Here the procedure for calculating the size distribution of the rock fragments once the individual rock particles have been delineated is briefly described. Calculating the size distribution for the test image shown in Fig. 1 allows a quantitative comparison between images delineated with the algorithms developed in this paper, and images delineated by hand.

For a volume of rock fragments, the size distribution is a plot of the cumulative percent of the volume greater than a certain fragment size, versus fragment size. The fragment "size" is a rather vague quantity. Since particle size distributions are normally calculated by screen sieving, an appropriate fragment size is the mesh size for the screen that will just allow the particle to pass. Using this definition, the fragment size should in some way be related to the intermediate and minimum dimensions of the fragment (i.e., fragments long in one direction can still pass through a small screen). Experiments conducted by

Kemeny *et al.* [18] on rock fragments of copper ore from southern Arizona show that a reasonable estimate for the screen size, S_i , of the i^{th} fragment is given by:

$$S_i = 0.45 \cdot a_i + 0.73 \cdot b_i$$

where a_i and b_i are the maximum and minimum diameter of the best-fitting ellipse for the i^{th} fragment. Also a reasonable estimate for the volume of the i^{th} particle is given by:

$$V_i = A_i \cdot S_i$$

where A_i is the area of the i^{th} particle. With the size and volume of each particle, the size distribution can be calculated. For the test image in Fig. 1, the size distribution calculated from the delineated particles from the procedure outlined in this paper is shown in Fig. 7. Also shown is the size distribution calculated when the particle delineation is performed by hand. Fig. 7 shows that the results compare very well.

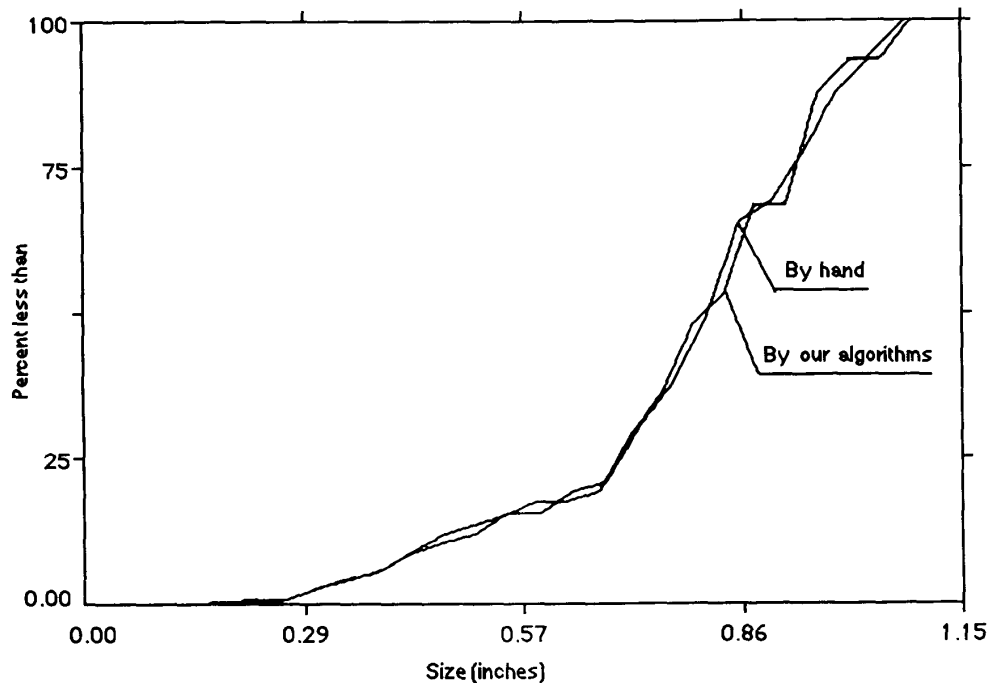


Fig. 7 Size distribution curves

VI. Discussion and Conclusions

A. Discussion

The procedure has trouble accurately delineating fragments under certain circumstances. For instance, if the light conditions are not uniform across the image, it is very difficult to obtain an optimal binary threshold value that preserves particle information across the whole image. This results in inaccuracies in the delineation of the individual particles. The use of an adaptive threshold to solve this problem is being studied at the present time. Also, under some circumstances, the surface of a rock fragment may be so rough that there are relatively large gradient paths across the fragment surface. In such an instance, the rock fragment may be split into two or more particles. The more sophisticated reasoning based on image evidence and particle shape knowledge is being studied.

For images containing fine particle areas (the diameter is less than 0.1 inch), our algorithm fails to delineate them. It is unlikely that any algorithm will be able to properly delineate the "fines". The best way to handle fine particle regions is to label them as fine areas. An image model

based on statistics and region growing is under study in order to intelligently distinguish background regions, fine particle regions, and multi-connected particle regions. The delineation algorithms will be only applied to the particle regions containing background regions.

B. Conclusions

The particle delineation procedure outlined in this paper is simple and accurate for images of fragmented rocks created by blasting. The algorithm has been tested on many images taken outdoors under sunlight and shade, underground subjected to low lighting conditions, and indoors under florescent lights. It is found that the algorithms are accurate and robust for fully multi-connected cases. The procedure is not sensitive to the general types of noise found in images of fractured rock (i.e., particle color changes, roughness on the surface of fragments, etc.). This makes the procedure superior to the present methods being used to delineate rock fragments in images of blasted rock.

The existing segmentation algorithms such as heuristic search, fuzzy set theory, region growing, and intelligent splitting are mainly for simply-connected particle

delineation problems. Based on Lemma 1, the paper proposes a new two-stage segmentation algorithm for fully multi-connected particle delineation. The first step is to extract simply-connected background regions separated by particles in images and find all possible links among background regions and make background regions multi-connected, and the particle regions then become simply-connected. The second step is to extract these simply-connected particle regions and find possible clusters of more than two touching particles and delineate them. We believe that this two-stage segmentation algorithm will be suitable for any multi-connected particle delineation problems in computer vision application areas.

Acknowledgments

This research has been supported by the Department of the Interior's Mineral Institutes program administered by the Bureau of Mines (grant number G1104104), by Cyprus Minerals Corporation under the supervision of Dr. James Savely (grant number C3593), and by the US Forest Service under the supervision of Bruce Vandre (grant number 4384M810310).

References

1. Clark, G.B., *Principles of Rock Fragmentation* John Wiley and Sons, NY, 606 pages (1987).
2. Franklin, J.A., Maerz, N.H., Bennett, C.P., Rock mass characterization using photoanalysis, *Int. J. Min. Geol. Eng.*, **6** 97-112 (1988).
3. Ghosh, A., Daemen, J.J.K., and van Zyl, D., Fractal based approach to determine the effect of discontinuities on blast fragmentation, *Proc. 31st US Rock Mechanics Symposium* Golden, CO (1990).
4. Mojtabai, N., Cetinas, A., Farmer, I.W., and Savely, J.P. In-palce and excavated block size distributions, *Proc. 30th Rock Mech. Symp.* Morgantown, WV, pp.537-543 (1989).
5. Maerz, N.H., Franklin, J.A., Rothenburg, L., and Coursen, D.L. Measurement of rock fragmentation using digital photoanalysis. *Proc. 6th Int. Cong. Rock Mech.* Montreal, Canada, **1**, 687-692 (1987).
6. Gao, Q.G. and Wong, A.K.C., Rock Image Segmentation, *Canada Image Interface* (1989).
7. J. E. Bowie and I. T. Young, An Analysis technique for biological shape-- *2 Acta Cytologica* **21** 455-464 (1977).
8. L. Vanderheydt, F. Dom, Two-dimensional shape decomposition using Fuzzy Subset Theory applied to automated chromosome analysis *Pattern Recognition* **13**, 147-157 (1981).
9. J. M. Chassery and C. Gaybay, An iterative segmentation method based on a contextual color and shape criterion *IEEE Trans. PAMI-6*, 794-800 (1984).
10. C. Gaybay, Image structure representation and processing: a discussion of some segmentation methods in cytology, *IEEE Trans. PAMI-8*, 140-146 (1986).
11. Liang Ji, Intelligent splitting in the chromosome domain, *Pattern Recognition*, **22** 519-532 (1989).
12. Russ, J.C. *Practical Stereology* Plenum Press, NY (1986).
13. Ian w. Farmer, John M. Kemeny, Analysis of rock fragmentation in bench blasting using digital image processing, *Proc. 6th Int. Cong. Rock Mech.* Aachen, Germany (1991).
14. Rafael C. Gonzalez, Paul Wintz, *Digital Image Processing* Adison-Wesley Publishing Company (1987).
15. D. H. Ballard and C. M. Brown, *Computer Vision* Prentice Hall, NJ (1982).
16. T. Pavlidis, A critical survey of image analysis methods, *Proc. IEEE ICPR-8* 502-511 (1986).
17. A. Rosenfeld and A.C. Kak, *Digital picture processing* pp. 371-372. Academic Press, NY (1976).
18. Kemeny, J.M., Devgan, A., Hagaman, R. and Wu, X.Q., Size distribution analysis using digital image processing (to be published).